IEICE TRANS. COMMUN., VOL.E98–B, NO.7 JULY 2015

PAPER Special Section on Electromagnetic Compatibility Technology in Conjunction with Main Topics of EMC'14/Tokyo

Dosimetry and Verification for 6-GHz Whole-Body Non-Constraint Exposure of Rats Using Reverberation Chamber

Jingjing SHI[†a)], **Jerdvisanop CHAKAROTHAI**[††b)], ***Members***, **Jianqing WANG**[†c)], ***Fellow***, **Kanako WAKE**[††], **Soichi WATANABE**[††], ***Members***, ***and*** **Osamu FUJIWARA**[†], ***Fellow***

SUMMARY With the rapid increase of various uses of wireless communications in modern life, the high microwave and millimeter wave frequency bands are attracting much attention. However, the existing databases on above 6 GHz radio-frequency (RF) electromagnetic (EM) field exposure of biological bodies are obviously insufficient. An *in-vivo* research project on local and whole-body exposure of rats to RF-EM fields above 6 GHz was started in Japan in 2013. This study aims to perform a dosimetric design for the whole-body-average specific absorption rates (WBA-SARs) of unconstrained rats exposed to 6 GHz RF-EM fields in a reverberation chamber (RC). The required input power into the RC is clarified using a two-step evaluation method in order to achieve a target exposure level in rats. The two-step method, which incorporates the finite-difference time-domain (FDTD) numerical solutions with electric field measurements in an RC exposure system, is used as an evaluation method to determine the whole-body exposure level in the rats. In order to verify the validity of the two-step method, we use *S*-parameter measurements inside the RC to experimentally derive the WBA-SARs with rat-equivalent phantoms and then compare those with the FDTD-calculated ones. It was shown that the difference between the two-step method and the *S*-parameter measurements is within 1.63 dB, which reveals the validity and usefulness of the two-step technique.

key words: *specific absorption rate (SAR), reverberation-chamber (RC) exposure system, finite-difference time-domain (FDTD) method, S-parameter measurements*

1. Introduction

Because of the wide uses of wireless devices and frequency extension of the signals, the higher microwave and millimeter wave frequency bands have been attracting special attention in recent years. Meanwhile, the potential risk to the human body and the biological effects related to the electromagnetic fields (EMF) exposure also have been raising intense public concerns. In response to growing public health concerns over possible health effects from exposure to an ever increasing number and diversity of EMF sources, the World Health Organization (WHO) launched a large, multidisciplinary research effort [1]. Based on a recent review of the scientific literature, the WHO concluded that current evidence does not confirm the existence of any health consequences from exposure to low level EMF. However, the fact is that the databases on above 6 GHz radio-frequency (RF) EMF exposure of biological bodies are obviously insufficient and further research is needed to fill these gaps.

The safety standards for human exposure to RF-EMF have been promulgated in various national or international guidelines worldwide to ensure the protection of humans against any effect of EMF exposure [2]. A whole-body-average-specific absorption rate (WBA-SAR), or a temporally and spatially averaged power deposited over the whole body mass, is used as a physical quantity of exposure assessment in view of the long-term base station EMF exposure. According to the International Commission on Non-Ionizing Radiation Protection (ICNIRP) guidelines, the WBA-SAR is restricted to 0.4 W/kg for occupational people, and 0.08 W/kg for general public with a reduction rate of 5 [3]. Studies using human volunteers provide valuable insight into the short term physiological effects of EMF exposure on humans, however, animal studies give opportunities to investigate the possible effects of long term EMF exposure, which cannot be conducted with human volunteers. As a result, in order to investigate the potential adverse biological effects, an animal experiment with high-quality exposure level quantification is indispensable in order to link a biological effect to the exposure level. This requires that the WBA-SAR be held at the designed level with the smallest variation possible throughout the animal experiment.

Reverberation chambers (RCs) are widely used for immunity tests involving electromagnetic compatibility (EMC). To simulate the electromagnetic (EM) environment inside an RC, different numerical approaches such as the finite-difference time-domain (FDTD) method, finite element method (FEM), method of moment (MoM), have been used [4]–[6]. In the last several years, RC-type exposure systems were developed for non-restrained small animal exposure experiments and have been adopted worldwide [7]–[9]. Due to the difficulty in WBA-SAR measurements, the SAR values are mainly calculated using numerical techniques. The most popular one is the FDTD method, which solves the Maxwell equations in a differential form. By linking the FDTD-calculated average SAR values to the electric field strength measured in an RC, an incident power related to the RC can be determined and regulated to achieve a requisite exposure level as done in [9]. We define the above method as "two-step method", in which the electric field measurement and FDTD simulation are combined together

Manuscript received October 10, 2014.
Manuscript revised February 12, 2015.

[†]The authors are with Nagoya Institute of Technology, Nagoya-shi, 466-8555 Japan.
[††]The authors are with National Institute of Information and Communication Technology, Koganei-shi, 184-0015 Japan.
a) E-mail: shi@nitech.ac.jp
b) E-mail: jerd@nict.go.jp
c) E-mail: wang@nitech.ac.jp

DOI: 10.1587/transcom.E98.B.1164

to determine the WBA-SAR for small animals in the RC. The two-step method consists of the following steps:

Step 1: measure the average electric field strength inside the RC with the small animals,

Step 2: calculate the SAR with numerical anatomical models by the FDTD simulation.

This two-step method avoids direct modeling of the RC in the FDTD simulation in which the convergence of the calculated fields is difficult to achieve. In the second step of the two-step method, the FDTD simulation for SAR calculation is on the basis of plane-wave superposition from various incident directions with random phases, which simulates an ideal EM environment with uniform field distribution in the RC [10]. Based on our previous investigations in [11], the validity of the two-step method was verified with the MoM approach, a totally numerical approach, using the same RC at 2 GHz for a whole-body exposure of mice. By comparing the physical quantities of the electric field strength inside the RC and the derived WBA-SARs for the anatomical mouse models, we found that the relative error of the two-step method to the MoM approach was approximately below 10%, which demonstrates its high accuracy. When the frequency changes from 2 GHz to 6 GHz, applying the MoM to the RC at such a high frequency needs too large computational burden, which implies further validation of the two-step method. We previously also proposed an *S*-parameter measurement technique to estimate the WBA-SAR in a human volunteer with an RC at 2 GHz, and the comparison results between the measured and the FDTD-calculated WBA-SARs revealed good agreements. As an experimental verification for the numerical dosimetry results of the above two-step method at 6 GHz for our RC, we try to use the *S*-parameter measurements to estimate the power absorbed by the rat-equivalent bodies, and then derive the WBA-SAR of the bodies to clarify the accuracy of the two-step method at 6 GHz. To the extent of authors' knowledge, this is the first time to experimentally verify the two-step method applied in the RC exposure system for whole-body exposure at 6 GHz.

In this study, we first try to employ *S*-parameter measurements in our developed RC exposure system at 6 GHz to experimentally verify the accuracy of the two-step method by comparing the WBA-SARs derived from the two-step method and the *S*-parameter measurements. Then, we dedicate ourselves to perform a quantitative dosimetric analysis with the two-step method and determine the required RC input power in order to achieve a target exposure level in rats.

This paper is organized as follows. In Sect. 2, we describe our developed RC-type exposure system, two-step method for SAR quantification, as well as *S*-parameter measurement technique to experimentally verify the two-step method. In Sect. 3, we show our measured and simulated results in the two-step method for homogeneous rat-equivalent phantoms, and then give an experimental verification by estimating the WBA-SARs in rat-equivalent phantoms to clarify the validity and accuracy of the two-step method. After the WBA-SAR verification, Sect. 4 gives a WBA-SAR quantification for inhomogeneous anatomical rat models in the RC at 6 GHz to link the antenna input power in our RC exposure system to the actual exposure level. Section 5 concludes this paper.

2. RC Exposure System and SAR Evaluation Methods

2.1 RC Exposure System

Figure 1 shows our developed RC exposure system for rats at 6 GHz. The system is composed of rotation controllers for the two stirrers, a signal generator (SG), a power amplifier, a PC for acquiring data and controlling the stirrers, a power meter, a directional coupler, and the RC. The RC consists of a rectangular enclosure and two stirrers, which are made of aluminum. The dimensions of the RC are 1.2 m × 1.0 m × 0.8 m. Both two stirrers "A" and "B" are installed almost vertically close to lateral wall and side wall, respectively, and each of the stirrers has a size of 64 cm × 24 cm. The two stirrers can be rotated with different degrees by a connected controller to make the electric field distribution inside the RC statistically uniform. An air filter is also installed to supply fresh air for animals confined in the RC to relieve their stress. A horn antenna available from 1 to 18 GHz was fixed inside the RC through the connector in the right-side wall. It radiated the EM wave toward a corner of the RC for avoiding the existence of a strong direct-wave component. A directional coupler with a coupling factor of 20 dB was used to connect the horn antenna and the power amplifier. By using the power meter, we can read the return loss from the antenna to obtain the input power to the RC. For the electric field strength measurements, a three-axis electric field probe (Narda, EP-600)

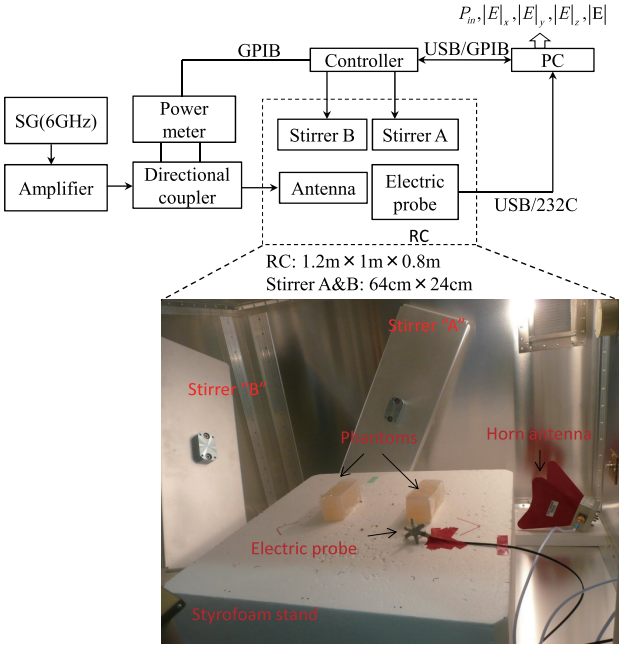

Fig. 1 RC exposure system for rats at 6 GHz.

was used to record the temporal electric field strength of $|E_x|$, $|E_y|$, $|E_z|$ and $|E|$ in the RC. A styrene foam with dimensions of 60 cm × 60 cm × 25 cm was placed in the RC as a working stand in order to arrange the exposure targets. The field uniformity, which was measured in accordance with IEC 61000 − 4 − 21 specification [12], was less than 3 dB for our designed RC.

2.2 Two-Step Method

The two-step method we employed in this study is composed of two steps. The first step is to measure the average electric field strength inside the RC, and the second step is to calculate the SARs with anatomically based numerical rat models by FDTD simulation.

2.2.1 Step 1: Measurement of Electric Field Strength

As the first step of the two step method to evaluate the WBA-SAR of biological bodies inside the RC, the average electric field strength should be measured in an actual RC exposure system with exposed biological bodies. The required electric field strength to produce a target SAR can be regulated by the antenna input power of the RC. By using our developed RC exposure system in Fig. 1, we measured the electric field strength inside the RC around the rat-equivalent homogeneous phantoms at 6 locations. Figure 2 shows an example of the detailed specifications and arrangements with two rat-equivalent phantoms on the styrofoam working stand. The interval distance of the two phantoms is 16 cm. In order to obtain a steady measured electric field strength, the distance between the measurement point and the phantom was fixed as 6 cm which is larger than one wavelength at 6 GHz. As discussed later based on the quality factor Q, the phantoms inside the RC are exposed in a uniformly distributed electric field environment. This implies that the arrangement of phantoms does not significantly affect the average value of the measured electric field strengths around the phantoms. Moreover, it has been shown in [6] that the influence from neighboring phantoms is almost ignorable when the distance between them is larger than one wavelength. So our measurements in the cases of one phantom, two phantoms, and four phantoms were only conducted at one placement pattern. Stirrer "A" was rotated counterclockwise from 0° to 353.5° with a 3.5° step angle in each turn of rotations, while stirrer "B" was rotated counterclockwise from 0° to 575.7° with a 5.7° step angle in each turn. During one round rotation, the measurements took five minutes approximately with 102 steps in total. The rat-equivalent phantoms made of agar, deionized water, polyethylene power, sodium chloride (NaCl), TX-151, and sodium azide (NaN_3), have a rectangular shape with dimensions of 5 cm × 5 cm × 11 cm and a weight of 300 g. The relative permittivity ε_r,conductivity σ and density ρ of the phantom were 32.77, 8.63 S/m, and 1000 kg/m^3, respectively, at 6 GHz. The measurement conditions in this study is summarized and tabulated in Table 1.

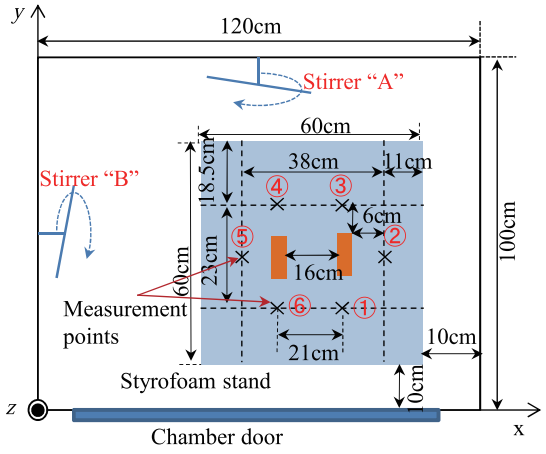

Fig. 2 Arrangements and detailed specifications for electric field measurement inside the RC exposure system.

Table 1 Electric field strength measurement conditions.

Frequency	6 GHz
Transmitting antenna	Horn antenna
Stirrer A	3.5° step, 0°~353.5°
Stirrer B	5.7° step, 0°~575.7°
Electric probe	3 axes, Narda, EP-600
Rotation steps	102 (5 minutes)
Measurement points	6
Rat-equivalent phantom	300 g, 5 cm × 5 cm × 11 cm, ε_r = 32.77, σ = 8.63 S/m,
Phantom number	0 (Empty), 1, 2, 4

2.2.2 Step 2: WBA-SAR Calculation

In the second step of the two-step method, to simulate the same situation as in the RC, we assume EM plane-waves irradiating from all directions with a constant electric field strength, since the exposure to the experimental animals in the RC could be considered as a far-field spherical irradiation under the ideal RC condition. Figure 3 shows EM plane-wave irradiations for two rat-equivalent phantoms with (a) E-polarization and (b) H-polarization. The incident direction of the EM plane-wave is defined by angles φ and θ. E-polarization irradiation is defined so as to have an electric field along the tangential direction of the longitude of the sphere, and a magnetic field along the tangential direction of the latitude of the sphere. H-polarization irradiation is defined so as to have a magnetic field along the tangential direction of the longitude of the sphere, and an electric field along the tangential direction of the latitude of the sphere. For complete simulation of an ideal RC, of course, all of the incident angle pairs should be taken into account to obtain the SAR values. However, we investigated the WBA-SARs with three to nine incident directions for our rat models. Based on the investigated results, the WBA-SARs of the rat models may reach a steady state as long as the incident number is over than 5 (with an angular interval of 72°), since the relative error with five, six, seven or eight incident

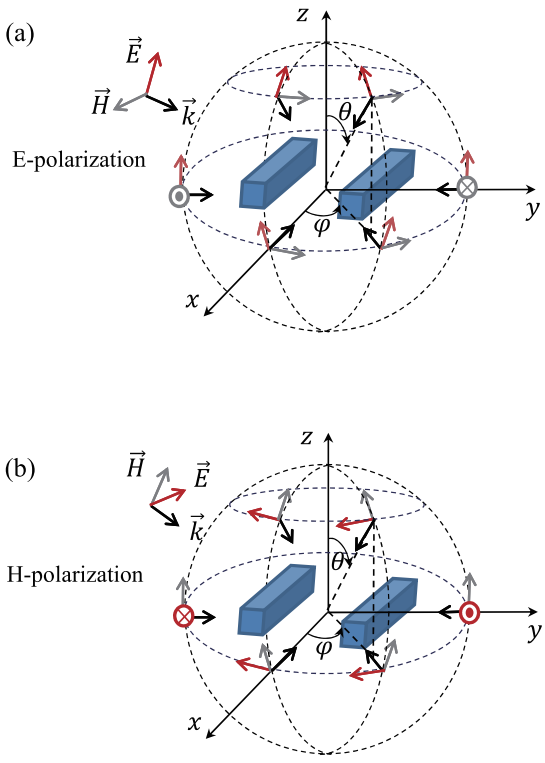

Fig. 3 EM plane-wave incidence in spherical form for simulating an ideal RC for two rat-equivalent phantoms with (a) E-polarization and (b) H-polarization.

directions was below 3% compared to that with nine incident directions.

In this study, we therefore employed a 40° interval of the angle of θ at the longitude direction and 80° interval of the angle of φ at the latitude direction, which results in 45 EM plane-wave irradiations with E-polarization and 45 EM plane-wave irradiations with H-polarization, respectively, and 90 EM plane-wave irradiations in total to calculate the WBA-SARs of the dielectric models inside the RC. In the FDTD calculations, we used perfectly matched layers (PML) of 12 layers as an absorbing boundary condition to avoid spurious reflections. The cell size was 1 mm × 1 mm × 1 mm, and the calculation lasts up to 16 periods of the sinusoidal waveform at 6 GHz until it reaches a steady state. In order to conduct the SAR verification with *S*-parameter measurements, we first used rat-equivalent phantoms which have the same dielectric properties and arrangements as those in the first step of the two step method to calculate the WBA-SARs by FDTD simulations. After clarifying the validity of the two-step method, we then employ the anatomical rat models to perform the WBA-SAR quantifications in our 6 GHz RC exposure system in Sect. 4.

2.3 S-Parameter Measurements for SAR Verification

According to [13], the absorbed power of the phantoms placed inside the RC $\langle P_{ab,p} \rangle$ can be derived as

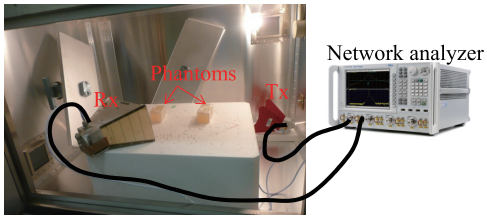

Fig. 4 Arrangement for measuring S_{11} and S_{21} with a network analyzer.

$$\left\langle P_{ab,p} \right\rangle = \left\langle P_{loss,p} \right\rangle \times \frac{S_{in}}{\left\langle S_{in,p} \right\rangle} - \left\langle P_{loss,e} \right\rangle \times \frac{S_{in}}{\left\langle S_{in,e} \right\rangle}. \quad (1)$$

Here, $\langle\rangle$ denotes the average during one period of a rotation cycle by the stirrers, and $\langle P_{loss} \rangle$ denotes the net dissipated power in the RC. When the RC is empty, the net dissipated power denoted as $\langle P_{loss,e} \rangle$ is mainly caused by the propagation loss or path loss and the Joule loss at the metal enclosure of the RC. However, if there are phantoms in the RC, the net dissipated power denoted as $\langle P_{loss,p} \rangle$ will contain not only the path loss and the Joule loss at the metal enclosure but also contain the power absorbed by the phantoms. Since the path loss and the Joule loss are different in these two cases, the absorbed power in the phantom cannot be simply defined as $\langle P_{loss,p} \rangle - \langle P_{loss,e} \rangle$. The terms of $\frac{S_{in}}{\langle S_{in,p} \rangle}$ and $\frac{S_{in}}{\langle S_{in,e} \rangle}$ are therefore portioned to $\langle P_{loss,p} \rangle$ and $\langle P_{loss,e} \rangle$, respectively, to derive the power absorbed only in the phantoms at the spatial power density S_{in}. $\langle S_{in,p} \rangle$ and $\langle S_{in,e} \rangle$ indicate the the spatially averaged power density with and without the phantom inside the RC, respectively, and they can be derived from the the squared electric field strength in the first step of the two step method in Sect. 2.2.1. Therefore, the WBA-SAR of the phantom at the spatial power density of S_{in} is determined by

$$\text{WBA-SAR} = \frac{\left\langle P_{ab,p} \right\rangle}{W}, \quad (2)$$

where W is the weight of the phantoms.

On the other hand, the net dissipated power in the chamber of $\langle P_{loss,e} \rangle$ and $\langle P_{loss,p} \rangle$ can be obtained by

$$\left\langle P_{loss,e} \right\rangle = \left\langle 1 - |S_{11,e}|^2 - |S_{21,e}|^2 \right\rangle P_i, \quad (3)$$

and

$$\left\langle P_{loss,p} \right\rangle = \left\langle 1 - |S_{11,p}|^2 - |S_{21,p}|^2 \right\rangle P_i. \quad (4)$$

Here, $S_{11,e}$ and $S_{11,p}$ correspond to the S_{11} parameters without and with the phantoms in the RC, respectively, $S_{21,e}$ and $S_{21,p}$ correspond to the S_{21} parameters without and with the phantoms in the RC, respectively, and P_i is the power supplied to the antenna. Figure 4 shows the arrangement for measuring S_{11} and S_{21} parameters. The transmitting and receiving antennas were arranged with different polarizations and without a direct path between them. Moreover, in order to remove the polarization influence of the antenna, we arranged the receiving antenna at two locations as can be seen in Fig. 5 and derived the average *S*-parameter results between them. A network analyzer was used outside the RC

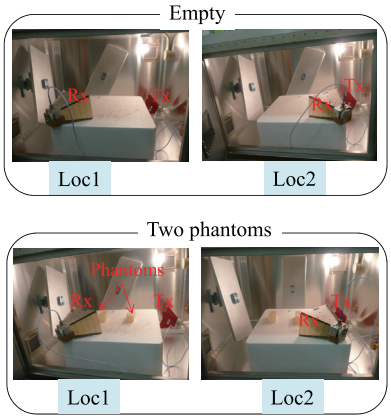

Fig. 5 Receiving antenna location in the measurements.

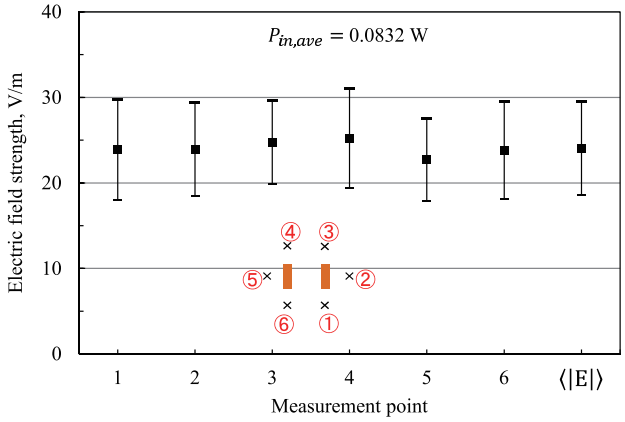

Fig. 6 Measured average electric field strength with two rat-equivalent phantoms.

to measure the S_{11} and S_{21} when the stirrers were rotating. The measurements were conducted during three rotation cycles of the stirrers, which spent approximately fifteen minutes.

3. Results and Discussions

3.1 Electric Field Strength

As shown in Fig. 1, the electric field strength was measured by means of a three-axis electric field probe at six locations which surrounded the rat-equivalent dielectric phantoms when the stirrers were rotating. The measurement were conducted in the case of one, two, and four rat phantoms inside the RC, as well as the case of empty. At each measurement point, we obtained the time-averaged electric field strength during one round of the stirrers rotating. The input power to the antenna was measured with the power meter when the stirrers were rotating, and the average value was found to be approximately 0.0827 W at 6 GHz.

Figure 6 shows an example of the time-averaged electric field strength and standard deviation at each measurement point with two rat-equivalent phantoms inside the RC. The standard deviation was indicated as bars. It can be seen that the time-averaged electric field strength for all the measurement points ranges from 22.71 V/m to 25.21 V/m, with the standard deviation from 4.87 V/m to 5.87 V/m. By using the time-averaged electric field strength at each measurement point, we furthermore obtained the spatial-average one denoted as $\langle|E|\rangle$ for all the measurement points and used it as an average electric field strength for the exposure evaluation. The mean values of the electric field strength and standard deviation were 24.07 V/m and 5.43 V/m, respectively, with the average antenna input power P_{in} of 0.0832 W.

The relationship between the spatial-average of the squared value of the electric field strength $\langle|E|^2\rangle$ and the antenna input power $P_{in} = (1 - |S_{11}|^2)P_i$ can be expressed as

$$\langle|E|^2\rangle = K\eta P_{in} \tag{5}$$

Table 2 Summary of the measured average electric field strength inside RC with P_{in} = 1 W.

Rat phantom number	Average electric field strength $\langle|E|\rangle$, V/m	Standard deviation, V/m
0 (Empty)	95.32	22.22 (23.3%)
1	89.38	20.56 (22.9%)
2	83.44	18.86 (22.6%)
4	77.5	17.28 (22.3%)

where K and η indicate a radiation coefficient and intrinsic impedance in the RC, respectively. It should be noted that in our RC $\langle|E|^2\rangle$ is found equal to $\langle|E|\rangle^2$ within a difference of 1%. We therefore use the expression $\langle|E|\rangle$ for $\sqrt{\langle|E|^2\rangle}$ hereafter. If we normalize the average input power P_{in} to 1 W, the average electric field strength produced inside the RC should be $\langle|E|\rangle$ = 83.44 V/m in the measurements. Similarly, we also obtained the statistical results of the electric field strength for the cases of one, four rat-equivalent phantoms arranged inside the RC, as well as the case of empty. It was found that in each case, the average electric field strength and its deviation were almost constant. With the increasing number of the rat phantoms, the measured average electric field strength becomes small compared to the case of empty. The summarized results for these cases are tabulated in Table 2 with a normalized antenna input power of P_{in} = 1 W. Based on these measured results, we then can take the temporally and spatially averaged electric field strength as the plane-wave incident electric field strength in the second step of the two-step method for determining the WBA-SAR with the FDTD simulation.

Moreover, we also calculated the quality factor Q of the RC using

$$Q = \frac{2\pi V\langle|E|^2\rangle}{P_{in}\mu_t\eta\lambda}, \tag{6}$$

where V is the volume of the RC, μ_t is the efficient factor of the transmitting antenna, and λ is the wavelength. Based on the measured electric field results in Table 2, the Q factors of the RC at 6 GHz were calculated as 2905 for the case of empty, 2555 for the case of one phantom, 2226 and 1921 for

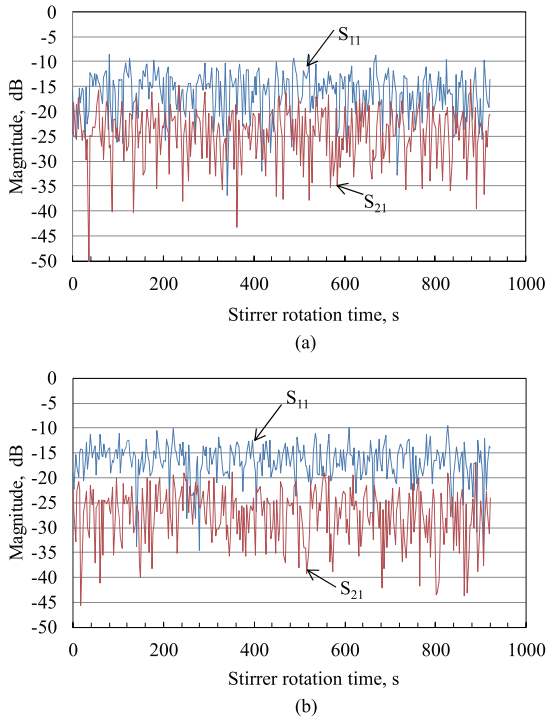

Fig. 7 *S*-parameter during stirrers rotation, (a) Empty (b) Two phantoms.

the cases of two and four phantoms, respectively. It reveals that all of the derived Q factors in this study are higher than 1000, which guarantees good field uniformity inside the RC [14].

3.2 WBA-SAR Verification

Figure 7 plots the measured *S*-parameter results when the RC is empty (a) and with two phantoms arranged inside the RC (b). This is the averaged result based on two receiving antenna locations as can be seen in Fig. 5. The magnitude of the *S*-parameter varied greatly according to the rotation of the stirrers. Due to the power absorbed in the phantoms, the difference of S_{11} and S_{21} is somewhat larger in (b) than that in (a). Moreover, the measured results including the *S*-parameter and net dissipated power are summarized in Table 3 based on Eqs. (3) and (4). The antenna input power was set as $P_{in} = 1$ W. As a result, using Eqs. (1) and (2) the measured WBA-SARs in the case of two phantoms can be derived as 0.0211 W/kg as shown in Table 4 at the spatial power density $S_{in} = 1\,\mathrm{W/m^2}$. Here, the power density $S_{in} = 1\,\mathrm{W/m^2}$ was obtained by assuming an electric field intensity of 19.42 V/m and a free-space intrinsic impedance of 377 Ω. The $\langle S_{in,p} \rangle$ and $\langle S_{in,e} \rangle$ were obtained from the squared values of the average electric field strength in Table 2 by dividing a free-space intrinsic impedance of 377 Ω.

On the other hand, in the two-step method, in the case with the two phantom models inside the RC, the WBA-SAR was calculated as 0.0145 W/kg for two phantoms at the spatial power density $S_{in} = 1\,\mathrm{W/m^2}$. The difference between the measured WBA-SAR and the two-step calculated

Table 3 Measured *S*-parameters and dissipate power in the RC at 6 GHz.

Phantom	$\langle \lvert S_{11} \rvert \rangle$	$\langle \lvert S_{21} \rvert \rangle$	P_{loss}, W
0	0.1676 (−15.5 dB)	0.0690 (−23.2 dB)	0.9609
2	0.1533 (−16.3 dB)	0.0499 (−26.0 dB)	0.9702

Table 4 WBA-SAR (W/kg) comparison for $S_i = 1\,\mathrm{W/m^2}$.

Measured WBA-SAR, W/kg	Two-step calculated WBA-SAR, W/kg	Difference, dB
0.0211	0.0145	1.63

WBA-SAR was approximately 1.63 dB. The comparison result is summarized in Table 4. Since IEEE recommends a ±2 dB uncertainty for practical SAR measurement in [15], the difference of 1.63 dB is within the range of allowable uncertainty in SAR measurement. As a result, it is acceptable to say that the measured and two-step calculated WBA-SARs are within a fair range, and the two-step method for SAR quantification in our develop RC system at 6 GHz is valid. The reasons about the difference between the two-step method and the S-parameter measurement method may be mainly attributed to the uncertainties in the electric field and S-parameter measurements, as well as the non-ideal performance of our developed RC at 6 GHz.

In addition, it should be noted that a key point to determine whether the RC or our evaluation method works well depends on the volume ratio of the RC to the rats. According to [13], as long as the volume of the RC is much larger than the volume of the living lossy body, i.e., 500 times larger, the RC can work well and the evaluation method can be clarified to be valid. In this study, we found that the volume of the RC was approximately 3000 times larger than the volume of four rats. Even though the rats get a little bit bigger, the volume ratio will not change significantly until it becomes smaller than 500. So our system and evaluation method should work well even though the rats get bigger or heavier during the exposure period.

4. WBA-SAR Quantification for Anatomical Rat Models

In previous chapter, the two-step method employed as a SAR quantification technique has been clarified to have an acceptable accuracy compared to the measured SAR result. In view of the difficulty in measuring the SAR in actual rats, we therefore perform a dosimetric analysis in our RC system at 6 GHz with anatomical rat models using the validated two-step method.

4.1 Rat Model

In order to accurately predict the whole-body exposure levels and the SAR distribution inside the actual rats, high-resolution anatomical models are essential for the dosimetric analysis. The numerical rat model employed in the WBA-SAR calculation in the RC was developed by National Institute of Information and Communication Tech-

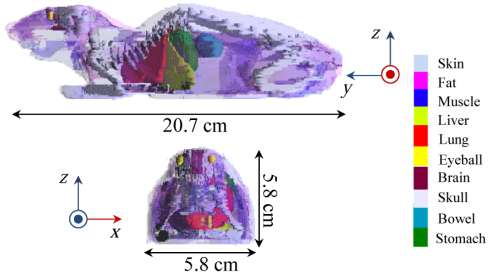

Fig. 8 Anatomical rat model.

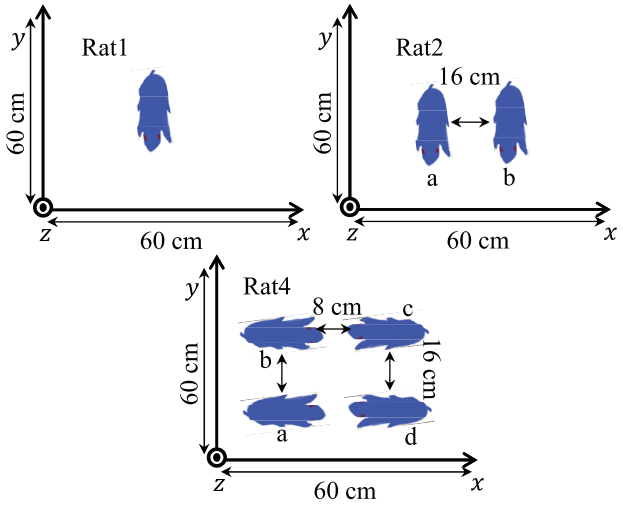

Fig. 9 Arrangements of the anatomical rat models.

nology (NICT), based on the magnetic resonance imaging (MRI) data of a living rat. As can be seen in Fig. 8, it was composed of ten tissue types including skin, fat, muscle, liver, lung, eyeball, brain, skull, bowel, and stomach with 1 mm resolution. Its maximum dimensions were 5.8 cm × 5.8 cm × 20.7 cm, and its weight was 300 g which is almost the same as the rat-equivalent phantom used in validating the two-step method. The dielectric constants at 6 GHz for the biological tissues of the rat model are cited from [16], in which the modeling was based on sample data from fresh animal and human autopsy materials.

4.2 WBA-SAR and Brain-Average SAR Results

Based on the FDTD simulation setting as described in Sect. 2.2.2, we derived the WBA-SARs and the brain-average SARs for one, two, and four anatomical rat model exposure. Figure 9 shows the arrangements in the second step of the two-step method for the cases of one, two, and four rat models, which accord with those in the electric field strength measurements in the first step of the two-step method. Generally, the SAR of the rat model is given by

$$\mathrm{SAR} = \frac{\sigma |E|^2_{internal}}{\rho} \tag{7}$$

where $|E|_{internal}$ is the root mean square value of the internal electric field strength of the rat model, σ is the conductivity and ρ is the density related to different type of tissues. The mean WBA-SAR in this study is defined as the average value of the individual WBA-SAR in each anatomical rat model. That is to say, after the WBA-SAR calculation of each rat model with the FDTD method, we furthermore derived the mean WBA-SAR for two and four rat models by means of dividing the total WAB-SARs by the rat numbers of two and four. Table 5 tabulates the derived WBA-SAR and the brain-average SAR results with the average incident electric field strength $\langle |E|_{in} \rangle = 1$ V/m in the FDTD numerical simulations. From this result, it can be observed that the mean WBA-SARs of one, two, and four rat models were almost at the same level of 0.051 mW/kg, and the brain-average SARs were about 1.4 times of the WBA-SARs when the average incident electric field strength was 1 V/m. Moreover, there is no large variation in the WBA-SAR of the rat model in each case since the standard deviation was found to be in a narrow range between 10.2% and 14.8%.

Table 5 WBA-SAR results for rat models with $\langle |E|_{in} \rangle = 1$ V/m.

Rat label	WBA-SAR, mW/kg (Std. deviation, %)	Brain-average SAR, mW/kg (Ratio to WBA-SAR)
Rat1	**0.0510, (10.2%)**	**0.0713, (1.40)**
Rat2(a)	0.0505, (11.4%)	0.0709, (1.40)
Rat2(b)	0.0509, (12.2%)	0.0730, (1.43)
Rat2(mean)	**0.0507, (11.8 %)**	**0.0719, (1.42)**
Rat4(a)	0.0502, (13.9%)	0.0710, (1.41)
Rat4(b)	0.0507, (14.8%)	0.0711, (1.40)
Rat4(c)	0.0509, (13.8%)	0.0719, (1.41)
Rat4(d)	0.0505, (14.2%)	0.0705, (1.40)
Rat4(mean)	**0.0506, (14.2%)**	**0.0711, (1.41)**

4.3 Exposure Level Quantification

By linking the FDTD-calculated mean WBA-SAR values to the electric field strength measured in an RC, an antenna input power related to the RC can be determined and regulated to achieve a requisite whole-body exposure level. Since the WBA-SAR is proportional to $\langle |E|^2 \rangle \fallingdotseq \langle |E| \rangle^2$, $\langle |E|_{req} \rangle$ can be simply obtained to achieve a target WBA-SAR from

$$\left\langle |E|_{req} \right\rangle = \sqrt{\frac{\mathrm{WBA\text{-}SAR}_{target}}{\mathrm{WBA\text{-}SAR}\big|_{\langle |E| \rangle = 1\ \mathrm{V/m}}}}. \tag{8}$$

Under the assumption that the ratio of the power deposited in the rat-equivalent phantom to the loss in the metal walls of the RC does not change with the antenna input power, when a target exposure level is given for the rats, a required input power $P_{in,req}$ or a required spatial-average electric field strength $\langle |E|_{req} \rangle$ related to the RC exposure system can be derived as

$$P_{in,req} = \frac{\left\langle |E|^2_{req} \right\rangle}{K\eta} \tag{9}$$

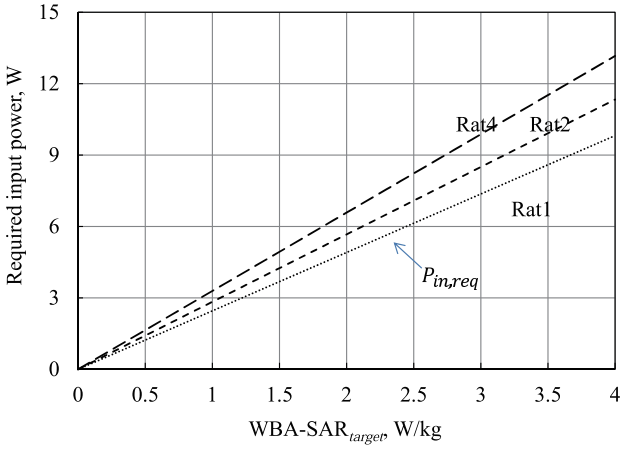

Fig. 10 Required input power versus WBA-SAR$_{target}$ for rats.

$$= \frac{\left\langle |E|^2_{req} \right\rangle}{\left\langle |E|^2_{req} \right\rangle\Big|_{P_{in}=1\,\mathrm{W}}} \tag{10}$$

$$= \frac{\text{WBA-SAR}_{target}}{\left\langle |E|^2_{req} \right\rangle\Big|_{P_{in}=1\,\mathrm{W}} \times \text{WBA-SAR}\Big|_{\langle |E| \rangle = 1\,\mathrm{V/m}}} \tag{11}$$

which is based on the proportional relationship in Eqs. (5) and (8). Here, $\langle |E|^2_{req} \rangle|_{P_{in}=1\,\mathrm{W}}$ indicates the spatial-average of the squared value of electric field strength produced in the RC when 1 W antenna input power is given, and $\text{WBA-SAR}|_{\langle |E| \rangle = 1\,\mathrm{V/m}}$ indicates the WBA-SAR value derived from FDTD calculations with 1 V/m plane-wave incident electric field strength.

As a result, by using the measured electric field strength results in Table 2 and the mean WBA-SAR results in Table 5, we derived the relationship of required antenna input power $P_{in,req}$ to achieve a target WBA-SAR or WBA-SAR$_{target}$ in our RC exposure system for rats as shown in Fig. 10. As can be seen in the figure, in order to achieve a WBA-SAR$_{target}$ of 4 W/kg, an antenna input power of 9.8 W should be required for one rat. If increasing the rat number, the corresponding required antenna input power should be increased to 11.3 W and 13.2 W for two and four rats, respectively. If the WBA-SAR$_{target}$ decreases to 0.4 W/kg, the required input power will be proportionally reduced to 0.98 W for one rat, 1.13 W and 1.32 W for two and four rat, respectively.

5. Conclusions

In this study, the validity of a two-step method, which combines electric field measurement with the FDTD solution to determine the WBA-SAR of rats in an RC exposure system at 6 GHz, has been verified by *S*-parameter measurement. The difference between the two-step method calculated and the *S*-parameter measured SARs has been clarified to be approximately within 1.63 dB. This result represents the first experimental confirmation of the validity of the two-step method at 6 GHz, although it has been used as a dosimetric tool in many RC exposure systems at lower frequencies. As a result, we used the two-step method in quantifying the exposure level quantification in an exposure experiment for rats using our RC exposure system. In order to realize a mean WBA-SAR in the rats of 4 W/kg (or 0.4 W/kg) in the RC exposure system at 6 GHz, the antenna input power should be 9.8 W (or 0.98 W) for one rat, 11.3 W (or 1.13 W) for two rats, and 13.2 W (or 1.32 W) for four rats.

Under the quantified whole-body exposure levels in such an approach, a large-scale animal experiment project for testing the possible biological effects at a frequency as high as 6 GHz has been started, and the corresponding findings will be reported in the near future.

Acknowledgment

This study was supported by the Ministry of Internal Affairs and Communications, Japan.

References

[1] World Health Organization, "2006 WHO Research Agenda for Radio Frequency Fields," WHO, Geneva, Switzerland, 2006.
[2] J.C. Lin, "Safety standards for human exposure to radio frequency radiation and their biological rationale," IEEE Microw. Mag., vol.4, no.4, pp.22–26, 2003.
[3] International Commission on Non-ionizing Radiation Protection, "Guidelines for limiting exposure to time-varying electric, magnetic, and electromagentic fields (up to 300 GHz)," Health Physics, vol.75, no.4, pp.494–522, 1998.
[4] F. Moglie and A.P. Pastore, "FDTD analysis of plane wave superposition to simulate susceptibility tests in reverberation chambers," IEEE Trans. Electromagn. Compat., vol.48, no.1, pp.195–202, 2006.
[5] C.F. Bunting, "Two-dimensional finite element analysis of reverberation chambers: the inclusion of a source and additional aspects of analysis," Proc. IEEE Internation. Symp. EMC, pp.219–224, Seattle, USA, Aug. 1999.
[6] J. Chakarothai, J. Wang, O. Fujiwara, K. Wake, and S. Watanabe, "Dosimetry of a reverberation chamber for whole-body exposure of small animals," IEEE Trans. Microw. Theory Techn., vol.61, no.9, pp.3435–3445, Sept. 2013.
[7] M. Capstick, N. Kuster, S. Kuhn, V. Berdinas-Torres, J. Ladbury, G. Koepke, D. McCormick, J. Gauger, and R. Melnick, "A radio frequency radiation reverberation chamber exposure system for rodents," Proc. of 29th URSI Gen. Assembly, Art. ID A07.4, 2008.
[8] P.F. Biagi, L. Castellana, T. Maggipinto, G. Maggipinto, T. Ligonzo, L. Schiavulli, and D. Loiacono, "A reverberation chamber to investigate the possible effects of in vivo exposure of rats to 1.8 GHz electromagnetic fields: a preliminary study," Progress in Electromagnetics Research, vol.94, pp.133–152, 2009.
[9] T. Wu, A. Hadjem, M.-F. Wong, A. Gati, O. Picon, and J. Wiart, "Whole-body new-born and young rats' exposure assessment in a reverberating chamber operating at 2.4 GHz," Phys. Med. Biol., vol.55, no.6, pp.1619–1630, 2010.
[10] D.A. Hill, "Plane wave integral representation for fields in reverberation chambers," IEEE Trans. Electromagn. Compat., vol.40, no.3, pp.209–217, 1998.
[11] J. Shi, J. Chakarothai, J. Wang, K. Wake, S. Watanabe, and O. Fujiwara, "Quantification and verification of whle-body-average SARs in small animals exposed to electromagnetic fields inside reverberation chamber," IEICE Trans. Commun., vol.E97-B, no.10, pp.2184–2191, Oct. 2014.

[12] IEC 61000-4-21 — Electromagnetic Compatibility (EMC) — Part 4-21: Testing and Measurement Techniques — Reverberation Chamber Test Methods, CISPR/A and IEC SC77B, IEC International Standard, Aug. 2003.
[13] J. Wang, T. Suzuki, O. Fujiwara, and H. Harima, "Measurement and validation of GHz-band whole-body average SAR in a human volunteer using reverberation chamber," Phys. Med. Biol., vol.57, no.23, pp.7893–7903, 2012.
[14] C.L. Holloway, D.A. Hill, J.M. Ladbury, and G. Koepke, "Requirements for an effective reverberation chamber: Unloaded or loaded," IEEE Trans. Electromagn. Compat., vol.48, no.1, pp.187–194, Feb. 2006.
[15] IEEE Std C95.3–2002, IEEE Recommended Practice for Measurements and Computations of Radio Frequency Electromagnetic Fields with Respect to Human Exposure to Such Fields, 100 kHz–300 GHz, 2002.
[16] C. Gabriel, "Compilation of the dielectric properties of body tissues at RF and microwave frequencies," Brooks AFB, San Antonio, TX, USA, books AFB Tech. Rep. AL/OE-TR-1996-0037, 1996.

Jingjing Shi received the B.E. degree from Shenyang University of Chemical Technology, Shenyang, China, in 2007, and the M.E. and D.E. degrees from Nagoya Institute of Technology, Nagoya, Japan, in 2010 and 2013, respectively. She is currently at Nagoya Institute of Technology as a Research Assistant Professor. Her research interests involve biomedical communications in wireless communication networks and biomedical EMC.

Jerdvisanop Chakarothai received his B.E. degree in electrical and electronic engineering from Akita University, Akita, Japan, in 2003, and his M.E. and D.E. degrees from Tohoku University, Sendai, Japan, in 2005 and 2010, respectively, both in electrical and communication engineering. He was a Research Associate at Tohoku University from 2010, prior to joining the Nagoya Institute of Technology, Nagoya, Japan, in 2011. He was a Research Associate at Tokyo Metropolitan University in 2013. He is currently with the National Institute of Information and Communications Technology, Tokyo, Japan. His research interests include computational electromagnetics (CEM) for biomedical communications and electromagnetic compatibility. Dr. Chakarothai is a member of IEEE.

Jianqing Wang received the B.E. degree in electronic engineering from Beijing Institute of Technology, Beijing, China, in 1984, and the M.E. and D.E. degrees in electrical and communication engineering from Tohoku University, Sendai, Japan, in 1988 and 1991, respectively. He was a Research Associate at Tohoku University and a Senior Engineer at Sophia Systems Co., Ltd., prior to joining Nagoya Institute of Technology, Nagoya, Japan, in 1997, where he is currently a Professor. His research interests include biomedical communications and electromagnetic compatibility.

Kanako Wake received the B.E., M.E., and D.E. degrees in electrical engineering from Tokyo Metropolitan University, Tokyo, Japan, in 1995, 1997, and 2000, respectively. She is currently with the National Institute of Information and Communications Technology, Tokyo, Japan, where she is involved in research on biomedical EM compatibility. Dr. Wake is a member of the Institute of Electrical Engineers, Japan, and the Bioelectromagnetics Society. She was the recipient of the 1999 International Scientific Radio Union Young Scientist Award.

Soichi Watanabe received the B.E., M.E., and D.E. degrees in electrical engineering from Tokyo Metropolitan University, Tokyo, Japan, in 1991, 1993, and 1996, respectively. He is currently with the National Institute of Information and Communications Technology, Tokyo, Japan. His main research interest includes biomedical EM compatibility. Dr. Watanabe is a member of the Institute of Electrical Engineers, Japan, the IEEE and Bioelectromagnetics Society. From 2004 to 2012, he was a member of the Standing Committee III on Physics and Engineering, International Commission on Non-Ionizing Radiation Protection (ICNIRP). He is a member of the main commission of ICNIRP since 2012. He was the recipient of the 1996 Young Scientist Award of the International Scientific Radio Union, the 1997 Best Paper Award of the IEICE, and the 2004 Best Paper Award (The Roberts Prize) of Physics in Medicine and Biology.

Osamu Fujiwara received the B.E. degree in electronic engineering from the Nagoya Institute of Technology, Nagoya, Japan, in 1971, and the M.E. and D.E. degrees from Nagoya University, Nagoya, Japan, in 1973 and 1980, respectively, both in electrical engineering. From 1973 to 1976, he was with the Central Research Laboratory, Hitachi Ltd., Kokubunji, Japan, where he was engaged in research and development of system packaging designs for computers. From 1980 to 1984, he was with the Department of Electrical Engineering, Nagoya University, as a Research Associate, and from 1984 to 1985, as an Assistant Professor. In 1985, he joined the Nagoya Institute of Technology, as an Associate Professor. In 1993, he became a Professor with the Graduate School of Engineering, Nagoya Institute of Technology. In 2012, he retired and became an Emeritus Professor with the Nagoya Institute of Technology. His research interests include measurement and control of EM interference due to discharge, bioelectromagnetics, and other related areas of EM compatibility. Dr. Fujiwara is a Fellow of the Institute of Electrical Engineers, Japan (IEEJ) and a member of the IEEE and Bioelectromagnetic Society.